STUDY ON ANALYSIS METHOD OF HORIZONTAL FLIGHT DISTANCE FOR ATM PERFORMANCE ASSESSMENT

Kota Kageyama , Yutaka Fukuda
Electronic Navigation Research Institute

Keywords: *Air Traffic Management, Key Performance Areas, Flight Efficiency*

Abstract

This paper describes an analysis method of flight distance for Japanese ATM (Air Traffic Management) performance assessment. The analysis method computes planned flight route length and actual flight distance. Planned flight routes/actual trajectories are divided into the three (3) parts; climb, cruise and descent. Flight distance is computed for each of the parts. The analysis method is applied to actual data of Japanese prime airport pairs and analysis results are presented. Compared to the great circle distance, planned route length proved to be extended in the climb/descent parts. Meanwhile, the extension in the climb parts proved to be mitigated in actual flight distance. As a result, compared to the great circle distance, actual flight distance is chiefly extended in the descent parts. Reduction of the flight distance in the descent part is indispensable for reduction of entire flight distance.

1 Introduction

To accommodate air traffic demand increase, ATM has significantly improved its performance in the last few decades. However, since higher quality of ATM service is required, further ATM performance improvements are required.

For that purpose, ATM performance evaluations are planned that will provide valuable performance assessment information. Through such ATM performance assessment, performance bottlenecks can be identified and prioritized in terms of severity in order to mitigate and hopefully remove them appropriately.

Since ATM has, by definition, multiple objectives to accomplish, its performance must be assessed from multiple viewpoints. For the definition of the various performance assessment viewpoints, ICAO (International Civil Aviation Organization) has defined Key Performance Areas (KPA)[1]. The KPA are comprised of 11 distinct areas related to societal impact (Safety, Security, Environment), ATM prosperity (Access and Equity, Participation by the ATM community), and ATM operational performance (Cost Effectiveness, Capacity, Efficiency, Flexibility and Predictability).

Flight distance is of importance from the view point of efficiency[2]. Since shorter flight distance should also contribute to reduction of fuel consumption and carbon dioxide emission, flight distance is closely related to the area of environment in the KPA. ATM has a fundamentally important role in reducing inefficiency in the paths flown by aircraft [3].

Studies on flight distance from the viewpoint of ATM performance have been conducted in some locations. In [4], flight efficiency was studied by comparing actual trajectory to the great circle distance between the origin and the destination airport as well as between exit of departure terminal circle and entrance into arrival terminal circle. In [5] and [6], flight efficiency in the United States and Europe was studied in a similar manner.

Each location has its specific character of air transport as well as ATM. Thus, ATM performance needs to be evaluated for each location.

The analysis method is hence studied and applied to Japanese actual data.

In addition to actual flight distance, planned route length is covered in this analysis method. The planned routes data do not include details to compute the route length [5]. Thus, the analysis method complements the detailed data for the computation. To study the relationship between flight phase and flight distance, planned routes/actual trajectories are divided into the three (3) parts and the distance is computed for each of the parts.

Firstly, the analysis method is introduced. Then, as an application instance, the analysis method is applied to actual data of Japanese prime airport pairs.

2 Analysis Method

2.1 Planned Flight Length

In many cases, airborne trajectory is comprised of the three (3) phases: SID (Standard Instrumental Departure), en-route, and STAR (Standard Terminal Arrival Route) including approach phase. The planned length L was hence computed as:

$$L = L_d + L_e + L_a, \tag{1}$$

where L_d , L_e and L_a represented SID, en-route and STAR length, respectively.

In the flight-plan, planned route which corresponded to L_e was described as a series of air routes and waypoints. Since air routes could be represented as a series of waypoints, L_e was computed as follows:

$$L_e = \sum_{i}^{n-1} s_{i,i+1}, \tag{2}$$

where $s_{i,i+1}$ represented the great circle distance between the waypoints $W_i (i = 1, 2, 3, \cdots, n-1)$ and W_{i+1} in the en-route part.

SID was assigned by ANSP (Air Navigation Service Provider) and recorded.

On the other hand, STAR was not recorded. With some arrival terminal ATC (Air Traffic Control), radar vectors are exploited instead of STARs. However, for the computation of L, L_a is indispensable. Thus, based on the final waypoints of the planned routes, R-NAV STARs that were usually shorter than the conventional ones were complemented.

SIDs and STARs included numerous curve elements and conditions were set for turning. As a result, it was difficult to compute the length solely based on waypoints distance. For the computation, the fast-time simulation software TAAM (Total Airport and Airspace Modeller) was exploited. Referring to the charts, SIDs and STARs were modeled on the software. Then, flights on the SIDs and STARs were simulated. TAAM had the function of trajectory recording of the simulated flights. L_d and L_a were determined from the recorded trajectories.

2.2 Actual Flight Distance

Actual flight distance was computed as follows. In the RDP (Radar Data Processing system) journals, coordinates of actual trajectories are recorded at 10 seconds intervals.

Actual flight distance M is computed as:

$$M = \sum_{i}^{n-1} d_{i,(i+1)}, \tag{3}$$

where $d_{i,(i+1)}$ represents the great circle distance between two successive coordinates of identical flight [7].

The Japanese radar coverage area was divided into four (4) areas and journals were recorded for each distinct area. To analyze flights over distinct areas, the journals were amalgamated. By amalgamating the journals, analyses of trajectories for the entire Japanese radar coverage areas were achieved.

2.3 Trajectory Division

Division of trajectories into some parts and comparison of the flight distance amongst the parts clarifies the characteristics of each part. Part division based on the operational phases (SID, en-route, STAR) is the most intuitive way, because

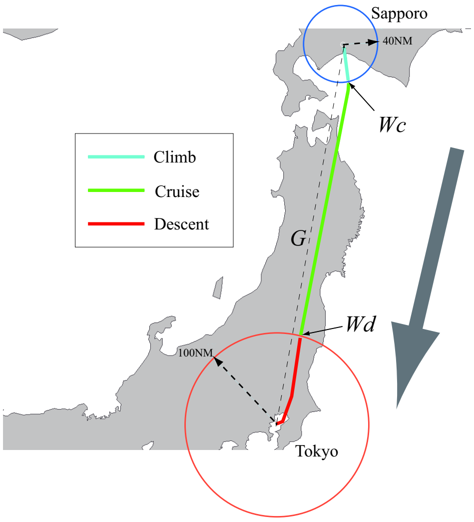

Fig. 1 The Part Division (RJCC→RJTT)

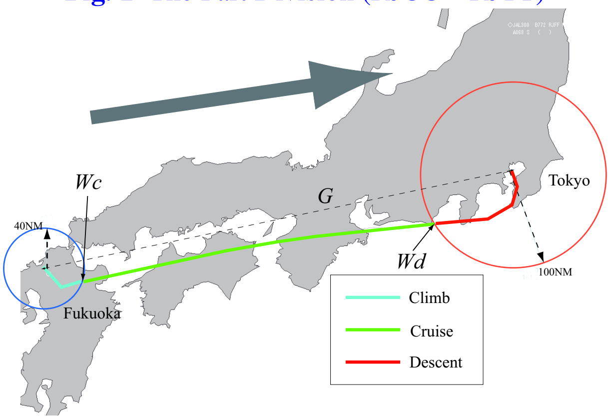

Fig. 2 The Part Division (RJFF→RJTT)

the division corresponds to the ATC procedure directly.

On the other hand, the dimension of origin and destination terminal ATC areas differs depending on the airports. For a strict comparison, constant dimensions should be defined amongst distinct airports.

In this analysis method, trajectory was divided into the three (3) parts: climb, cruise and descent. Along with PRR (Performance Review Report) [8], climb was defined as the part within a radius of 40NM around the origin airport; descent was defined as the part within a radius of 100NM around the destination airport.

At the same time, en-route was defined as the rest of the airborne trajectory; the en-route part definition was different from PRR's one that corresponded to segment route between departure and arrival terminal circles with a radii of 40NM. The analysis method divides the route explicitly to compare the flight distance amongst the parts.

Based on this definition, planned routes were divided into the three (3) parts. The lengths of the divided routes were respectively described as L_u (climb), L_c (cruise) and L_d (descent). Because the planned route should be compared to the great circle path, the indices of the route length were defined as follows:

$$\Delta L_u = L_u - 40 \qquad \text{(climb)}, \qquad (4)$$
$$\Delta L_c = L_c - G_c \qquad \text{(cruise)}, \qquad (5)$$
$$\Delta L_d = L_d - 100 \qquad \text{(descent)}. \qquad (6)$$

Here, G_c represents the great circle distance between the intersections of the planned routes and the two (2) radii (40NM around the origin airport and 100NM around the destination airport).

Actual airborne trajectory was divided into the three (3) parts in the same manner as the planned route. The lengths of the parts were respectively described as M_u (climb), M_c (cruise) and M_d (descent). Because the actual airborne trajectory should be compared to to the planned route, the indices of the flight distance were defined as follows:

$$\Delta M_u = M_u - L_u \qquad \text{(climb)}, \qquad (7)$$
$$\Delta M_c = M_c - L_c \qquad \text{(cruise)}, \qquad (8)$$
$$\Delta M_d = M_d - L_d \qquad \text{(descent)}. \qquad (9)$$

3 Application Instances

3.1 The Analyzed Data Set

Application scenarios of the analysis method are presented in the remainder of this paper. Amongst Japanese airport pairs, Tokyo (RJTT) - Fukuoka (RJFF) and Tokyo - Sapporo (RJCC) were regarded as the prime ones in Japan. RJTT played the role of a domestic hub airport in Japan. Actual data of the airport pairs were analyzed.

The ANSP announces recommended routes for the airport pairs. Fig. 1 and Fig. 2 show examples of the recommended routes and corresponding part division. In the figures, W_c represents the intersection between the route and a ring of 40NM radius around the origin airports; W_d represents intersection between the route and a ring of 100NM radius around the destination airports. The great circle distance between W_c and W_d corresponds to G_c. At the same time, G represents the great circle distance between the origin and the destination airports.

The flights for which planned routes were identical to the recommended ones were extracted and analyzed. RDP and FDMS (Flight Data Management System) journals were exploited to retrieve the data items. Seven (7) days worth of data recorded in February 2007 were gathered. The data covered 358 flights (RJTT→RJCC), 368 flights (RJCC→RJTT), 316 flights (RJTT→RJFF) and 304 flights (RJFF →RJTT).

Because SIDs and STARs differed depending on runways, actual used runways were obtained from the trajectories. Then, SIDs and STARs corresponding to the runways were assigned to determine L_d and L_a.

3.2 A Study on Planned Flight Length

Figures 3, 4, 5 and 6 show the averages of ΔL_u, ΔL_c and ΔL_d for each route. As ΔL_u and ΔL_d differed depending on the used runways, the averages of ΔL_u and ΔL_d were computed for each of the distinct take-off/touch-down runways. Table 1 shows usage rate of the runways in the analyzed data set.

From the figures, it was observed that ΔL_c was considerably lower than ΔL_u and ΔL_d. It was also observed that ΔL_u and ΔL_d could differ drastically depending on the runways (e.g. Fig. 3).

Alignment of take-off runway orientation angle and W_c had an impact on ΔL_u: In the case of W_c reversing the runway orientation angle, ΔL_u is extended. Alignment of touch-down runway orientation angle and W_d had an impact on ΔL_d in a similar fashion.

On the other hand, Fig. 4 and Fig. 6 indicate that regardless of touch-down runway usage, ΔL_d

Table 1 Usage Rate of the Runways

City-pair	Category	Runway	%
RJTT→RJCC	Take-off	16R	21
		34R	79
	Touch-down	01R	85
		19L	15
RJCC→RJTT	Take-off	01L	85
		19R	15
	Touch-down	16L	21
		34L	79
RJTT→RJFF	Take-off	16R	25
		34R	75
	Touch-down	16	82
		34	18
RJFF→RJTT	Take-off	16	87
		34	13
	Touch-down	16L	23
		34L	77

of RJTT arrivals was longer.

3.3 A Study of Actual Flight Length

For the same data set, actual flight distance was examined. Figures 7, 8, 9 and 10 show the averages of ΔM_u, ΔM_c and ΔM_d for each route. The averages of ΔM_u and ΔM_d were computed for each of the take-off/touch-down runways.

In the figures, it was observed that the actual flight distance was shorter than the planned route distance in some cases. This implies that some of the corresponding flights were given direct routes. As a result, the extended distance of the planned routes could be compensated to some extent.

ΔM_d tended to be higher than the others, which implied that actual flight distance was increased in the descent part.

Figures 11, 12, 13 and 14 represent frequent distribution of ΔM_u. From the figures, different averages of ΔM_u depending on take-off runways were confirmed. In the case of the runway orientation angle requiring turning (e.g. Runway 16R in Figure 11, Runway 34R in Figure 13), ΔM_u got shorter. It implied direct routing in the turning part.

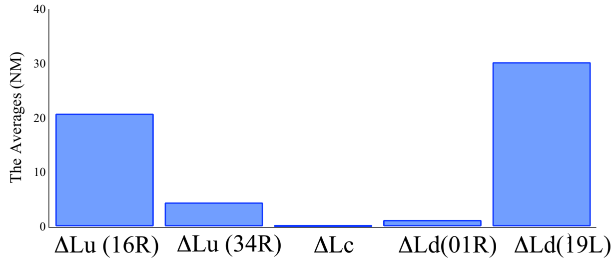

Fig. 3 The Averages : RJTT→RJCC

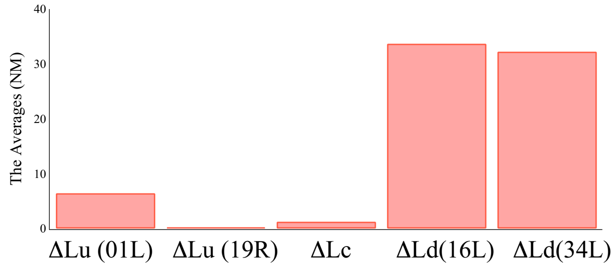

Fig. 4 The Averages : RJCC→RJTT

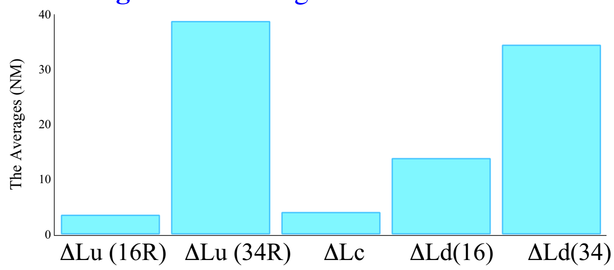

Fig. 5 The Averages : RJTT→RJFF

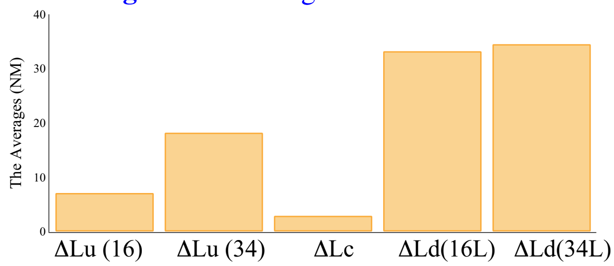

Fig. 6 The Averages : RJFF→RJTT

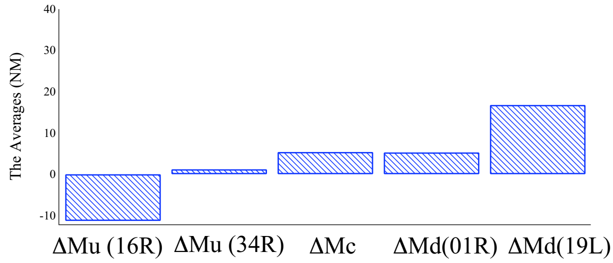

Fig. 7 The Averages : RJTT→RJCC

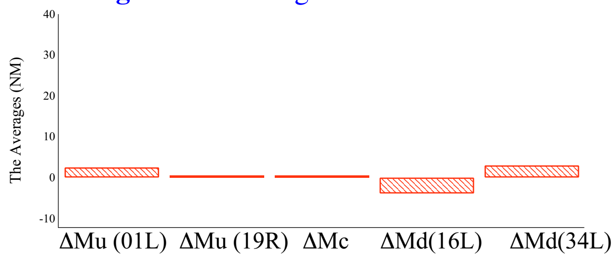

Fig. 8 The Averages : RJCC→RJTT

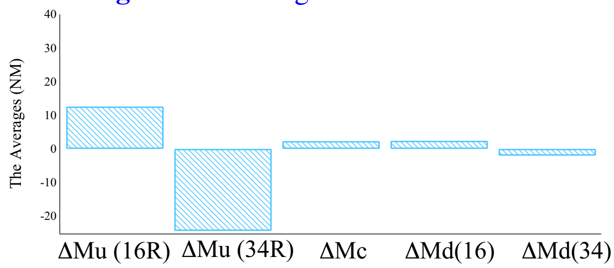

Fig. 9 The Averages : RJTT→RJFF

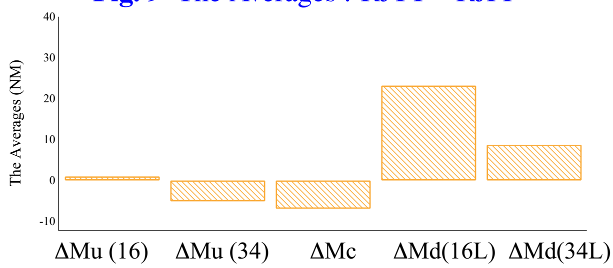

Fig. 10 The Averages : RJFF→RJTT

Figures 15, 16, 17 and 18 represent frequent distribution of ΔM_d. From the figures, different averages of ΔM_d depending on touch-down runways were confirmed.

In addition, although negative values corresponding to direct routings were found, there was an extensive range of ΔM_d values. This was attributed to the nature of the descent part. In the descent part, an arrival flow in which arrivals maintained adequate separation needed to be formed. For the flow formation, extra flight distance was required for the adjustment of separation between arrivals.

Fig. 19 shows a comparison of the entire flight distance averages. In this figure, the great circle distance between the origin and the destination airports(G), the entire planned route length(L) and the entire actual flight distance(M) are compared for each of the routes. Table 2 shows the ratio of L and M to G. The actual flight

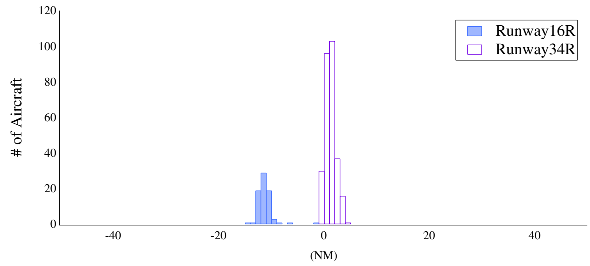

Fig. 11 Distribution of ΔM_u : RJTT→RJCC

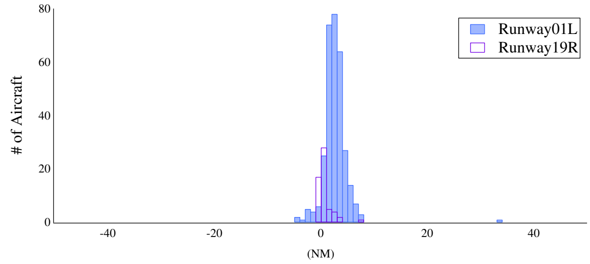

Fig. 12 Distribution of ΔM_u : RJCC→RJTT

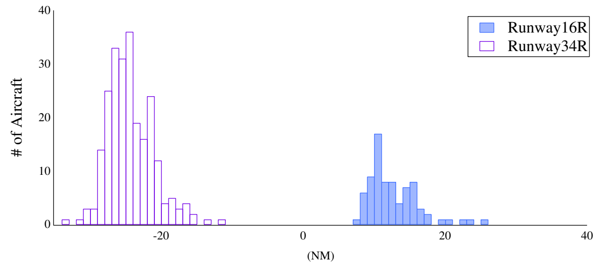

Fig. 13 Distribution of ΔM_u : RJTT→RJFF

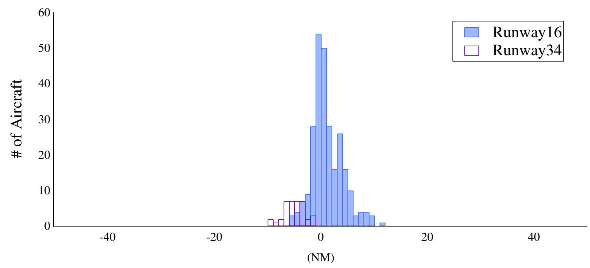

Fig. 14 Distribution of ΔM_u : RJFF→RJTT

distance M ranged from 105% to 116% of great circle distance G. On the whole, L/G was virtually equivalent to M/G. That is, the increase of actual flight distance was mainly attributed to the increase in the planned length.

3.4 Discussion

To compare actual flight distance with the great circle distance, the following indices were de-

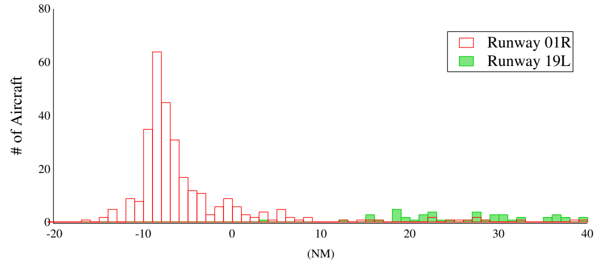

Fig. 15 Distribution of ΔM_d : RJTT→RJCC

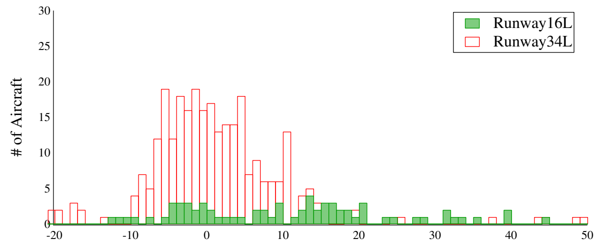

Fig. 16 Distribution of ΔM_d : RJCC→RJTT

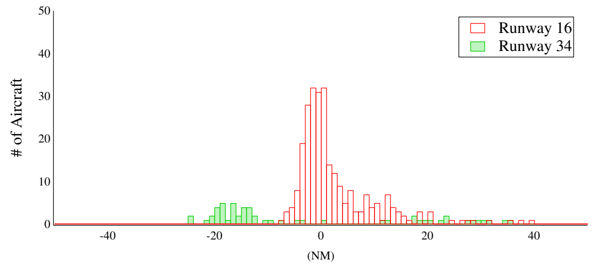

Fig. 17 Distribution of ΔM_d : RJTT→RJFF

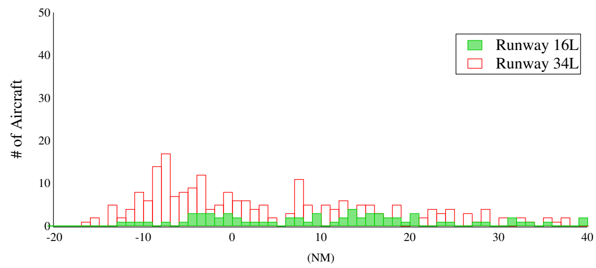

Fig. 18 Distribution of ΔM_d : RJFF→RJTT

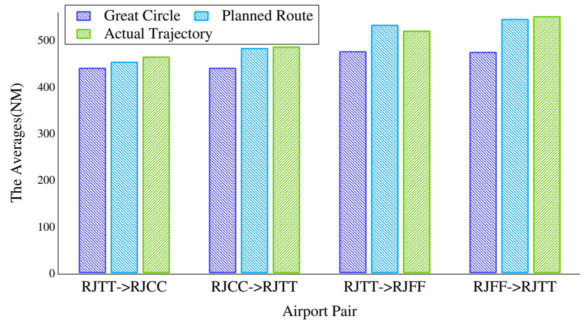

Fig. 19 The Averages of L, M and G

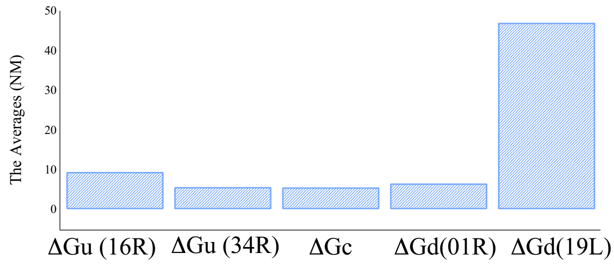

Fig. 20 The Averages : RJTT→RJCC

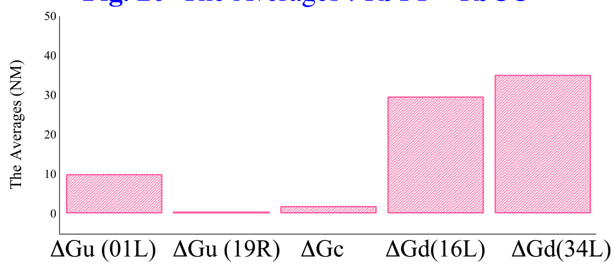

Fig. 21 The Averages : RJCC→RJTT

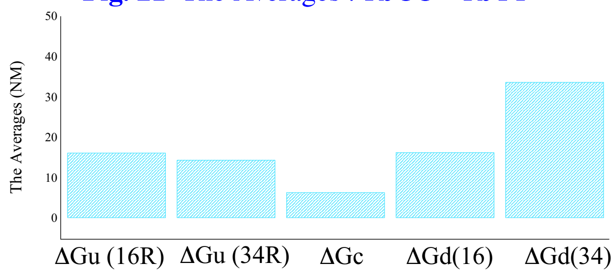

Fig. 22 The Averages : RJTT→RJFF

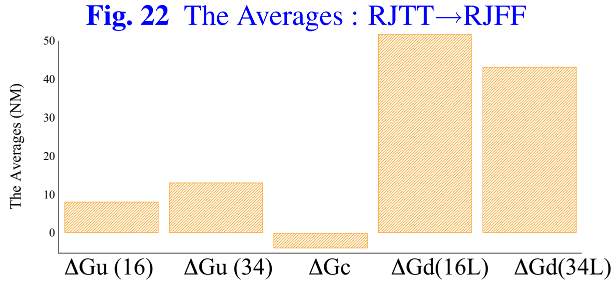

Fig. 23 The Averages : RJFF→RJTT

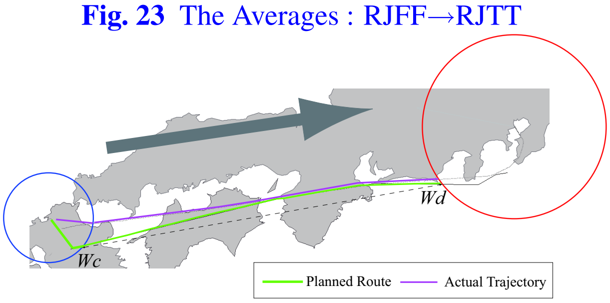

Fig. 24 An Example of Shortcut : RJFF→RJTT

Table 2 The Ratio of L and M

Airport Pair	L/G	M/G
RJTT → RJCC	1.03	1.05
RJCC → RJTT	1.10	1.10
RJTT → RJFF	1.12	1.09
RJFF → RJTT	1.15	1.16

fined:

$$\Delta G_u = M_u - G_u \quad \text{(climb)}, \tag{10}$$
$$\Delta G_c = M_c - G_c \quad \text{(cruise)}, \tag{11}$$
$$\Delta G_d = M_d - G_d \quad \text{(descent)}. \tag{12}$$

Figures 20, 21, 22 and 23 show the averages of the index values. In the figure, ΔG_c tended to be rather small; ΔG_d tended to be larger.

As it was indicated in Figures 3, 4, 5 and 6, the planned routes were extended in the climb/descent parts. Meanwhile, as it was indicated in Figures 7, 8, 9 and 10, the actual flight distance tended to be shortened in the climb part.

On the other hand, the actual flight distance tended to be further extended in the descent part. As mentioned in 3.3, it was due to arrival flow formation. Adjustment of arrival time before arrivals enter into the descent part should reduce the extra flight distance in the part.

As it was indicated in Fig. 16, and Fig. 18, the distribution of ΔM_d for RJTT arrivals was particularly large.

It should be noted that G_c averaged negative in Fig. 23. This was attributed to direct routing over climb and cruise parts. Fig. 24 represents the idea of the direct route. In the figure, flight in the climb part was given a shortcut to a point of the cruise part. As a result, the actual trajectory in the cruise part got even shorter than the great distance path between W_c and W_d.

4 Conclusions

This paper presented an analysis method of flight distance. For the computation of detailed planned flight distance, the analysis method complemented STAR to the data items in flight-plans.

Application instances of the analysis method were then presented. From the comparison between the great circle distance and planned flight length, it was observed that planned flight length was extended in the climb/descent part and planned flight route length was considerably close to the great circle distance in the cruise part. It was also confirmed that runway usage had an impact on the planned flight route length in the climb/descent part.

On the other hand, it was indicated that although it was shortened in the climb/cruise part, actual flight distance tended to be further extended in the descent part. Reduction of the flight distance in the descent part is indispensable for reduction of entire flight distance.

There can be no doubt that flight distance need to be analyzed for the other period and airport pairs to achieve a detailed ATM performance analysis. Continuous application of the data analysis method presented in this paper can assist in monitoring and controlling flight distance and consequently offer significant insights into future ATM improvements.

Acknowledgements

The authors are grateful to JCAB (Japan Civil Aviation Bureau), Ministry of Land, Infrastructure and Transport and Tourism, Japan for their cooperation in the acquisition of the actual performance data. In particular, many thanks go to Mr. Kimihiko Itoh and Mr. Ryo Yamauchi for their cooperation.

The authors also would like to thank Mr. Kazuo Akinaga and Mr. Yoshihiro Miyatsu for their continuing support and useful advice.

Contact Author Email Address

kage@enri.go.jp

Copyright Statement

References

[1] ICAO Global air traffic management operational concept. Doc 9854 AN/458, 2005.

[2] Performance Review Commission Performance review report 2007. Eurocontrol, 2008.

[3] Reynolds T. G. Development of flight inefficiency metrics for environmental performance assessment of ATM. *Proc 8th USA/Europe ATM R&D Seminar*, 2009.

[4] Dan Howell, Michael Bennett, James Bonn and David Knorr Estimating the en route efficiency benefits pool. *Proc 5th USA/Europe ATM R&D Seminar*, 2003.

[5] Tarja Kattunen, Jean-Claude Hustache, Ian Fuller, Dan Howell, James Bonn and Dave Knorr Flight efficiency studies in Europe and the United States. *Proc 6th USA/Europe ATM R&D Seminar*, 2005.

[6] James Gulding, David Knorr, Marc Rose, James Bonn Philippe Enaud and Holger Hegendoerfer US/Europe comparison of ATM-related operational performance. *Proc 8th USA/Europe Air Traffic Management Research and Development*, 2009.

[7] Yutaka Fukuda, Kota Kageyama Measurement and analysis of flight distance from actual operational data *Proc 2008 KSAS-JSASS Joint International Symposium on Aerospace Engineering*, 2008.

[8] Performance Review Commission Performance review report 2008. Eurocontrol, 2009.